View metadata, citation and similar papers at core.ac.uk

brought to you by CORE

provided by Elsevier - Publisher Connector

Energy Conversion and Management 125 (2016) 336–346

Contents lists available at ScienceDirect

Energy Conversion and Management

journal homepage: www.elsevier.com/locate/enconman

Backup flexibility classes in emerging large-scale renewable electricity systems

D.P. Schlachtberger [a,*], S. Becker [a], S. Schramm [a], M. Greiner [b]

[a] Frankfurt Institute for Advanced Studies, 60438 Frankfurt am Main, Germany
[b] Department of Engineering, Aarhus University, 8000 Aarhus C, Denmark

ARTICLE INFO

Article history:
Received 16 November 2015
Received in revised form 1 April 2016
Accepted 4 April 2016
Available online 12 April 2016

Keywords:
Energy system design
Large-scale integration of renewable power generation
Flexible backup power
Wind power
Solar power

ABSTRACT

High shares of intermittent renewable power generation in a European electricity system will require flexible backup power generation on the dominant diurnal, synoptic, and seasonal weather timescales. The same three timescales are already covered by today's dispatchable electricity generation facilities, which are able to follow the typical load variations on the intra-day, intra-week, and seasonal timescales. This work aims to quantify the changing demand for those three backup flexibility classes in emerging large-scale electricity systems, as they transform from low to high shares of variable renewable power generation. A weather-driven modelling is used, which aggregates eight years of wind and solar power generation data as well as load data over Germany and Europe, and splits the backup system required to cover the residual load into three flexibility classes distinguished by their respective maximum rates of change of power output. This modelling shows that the slowly flexible backup system is dominant at low renewable shares, but its optimized capacity decreases and drops close to zero once the average renewable power generation exceeds 50% of the mean load. The medium flexible backup capacities increase for modest renewable shares, peak at around a 40% renewable share, and then continuously decrease to almost zero once the average renewable power generation becomes larger than 100% of the mean load. The dispatch capacity of the highly flexible backup system becomes dominant for renewable shares beyond 50%, and reach their maximum around a 70% renewable share. For renewable shares above 70% the highly flexible backup capacity in Germany remains at its maximum, whereas it decreases again for Europe. This indicates that for highly renewable large-scale electricity systems the total required backup capacity can only be reduced if countries share their excess generation and backup power.

© 2016 The Authors. Published by Elsevier Ltd. This is an open access article under the CC BY-NC-ND license (http://creativecommons.org/licenses/by-nc-nd/4.0/).

1. Introduction

The dispatchable electricity generation facilities that are widespread today were mainly constructed with the aim of matching demand requirements. They split more or less into three flexibility classes, which are able to follow the typical load variations on the intra-day, intra-week, and seasonal timescales; see Fig. 1. During the day, variations in the load are usually due to human activity. Furthermore, the load is reduced during weekends and public holidays, and seasonal changes lead to higher load in the winter due to longer nights and increased heating demand. Examples of current slowly flexible generators are nuclear and lignite power plants, coal and combined-cycle gas power plants are medium flexible, and open-cycle gas turbines are highly flexible.

This mix of conventional power generation plants is going to change. In order to mitigate the negative impact of climate change, some countries (like Germany and Denmark) are following ambitious targets on reducing CO_2 emissions and on increasing the integration of renewable energies [2]. Both targets pressure the existence of some of the conventional power plants, in particular the lignite and coal power plants. As to the second target, the increasing share of weather-driven variable renewable energy sources (VRES) – mainly wind and solar PV power – poses new challenges, and in particular leads to an increase in fluctuations of the residual load. This requires more highly flexible backup power plants. Slowly flexible power plants will be less needed, but phasing them out too early might turn out to be a mistake.

In highly renewable electricity systems the same three flexibility timescales as in the conventional power systems are also present [1]. They are determined by the weather variations which cause the wind and solar power generation to fluctuate. The

* Corresponding author.
E-mail address: schlachtberger@fias.uni-frankfurt.de (D.P. Schlachtberger).

http://dx.doi.org/10.1016/j.enconman.2016.04.020
0196-8904/© 2016 The Authors. Published by Elsevier Ltd.
This is an open access article under the CC BY-NC-ND license (http://creativecommons.org/licenses/by-nc-nd/4.0/).

Nomenclature

VRES	variable renewable energy sources	i	flexibility class
PV	photovoltaics	m_i	maximum rate of change
DE	Germany	$B_i(t)$	power output
Agg.	aggregated Europe	K_i	power capacity
av.l.h.	average load hours	K_{tot}	total power capacity
T	total number of hours	c, w_i	capacity weight parameters
t	specific hour of the time series	d, v_i	dispatch weight parameters
$L(t)$	load	E_{miss}	missing energy
$\langle L \rangle$	mean load	E_{excess}	excess energy
$L_R(t)$	residual load	f_i	utilization fraction
$W(t)$	wind generation	Φ	optimization function
$S(t)$	solar generation	q	quantile of fully covered hours
γ	gross share of VRES	N_{miss}	number of partly covered hours
α	wind fraction		

intra-day timescale is called the diurnal timescale and is most clearly seen in the solar power generation following the availability of sunlight; see again Fig. 1. Wind variations are dominated by synoptic weather patterns in Europe, which fluctuate on the timescale of three to ten days [3]. These weekly fluctuations also have an effect on the solar irradiation and thus the solar photovoltaic (PV) production. Finally, seasonal changes are observed, with typically more wind power production and less solar PV generation in winter and vice versa in summer.

To include a large share of variable renewable energy, the energy system has to become more flexible. There is a considerable spread in the interpretation of what flexibility in the electricity system actually means, ranging from the more direct definition of the ability to react to variability, e.g., [4], and uncertainty of forecasts of variable generation [5], to more indirect policy, regulation, and market implementation issues of making balancing energy and power available, e.g., [6]. Depending on the complexity of the modelled system, different flexibility metrics have been proposed or reviewed. Metrics based purely on the properties of the residual load at given shares of variable generation are defined by Tarroja et al. [7]. They allow insight into principal properties of the flexibility requirements of the dispatchable part of an energy system. In a similar setting, Huber et al. [8] focus on flexibility needs based on (residual) load gradients over different time intervals and spatial scales in Europe. Additional metrics can be defined in dispatch simulations, e.g., to measure the difference between forecast and actual (residual) load [9], missing or surplus energy, or missing or surplus power [10] (see [11] for a comprehensive summary). These also include different metrics for the (in-) sufficiency of flexibility in the systems, such as the loss of load expectation or the number of unserved hours [9]. This study concentrates on the challenges posed by ramp rates in the residual load, measuring the quality of the flexible system in terms of unserved energy.

Dispatchable generators are not the only possible source of flexibility. Recent studies considered the influence of storage (e.g., [12]), transmission grid extension (e.g., [13]), demand-side-management, curtailment, system integration with the heating (e.g., [14]) and transport sector (e.g., [15]), economic efficiency (e.g., [16]), forecast errors, and combinations thereof. Kondziella and Bruckner [17] provide a thorough review of different technical, economic, and market based modelling approaches and requirements for the different aspects of flexibility demand. A range of more specialized flexibility metrics for these options is reviewed by Østergaard [18].

This paper analyses a stylized model of the European electricity system, consisting of weather-based wind and solar PV generation and historical load data from Ref. [1] with hourly resolution. These are assumed to be complemented by dispatchable generation of three flexibility classes, which are designed to follow the load and the renewable power generation on the diurnal, synoptic, and seasonal timescales, respectively. To define the three flexibility classes, maximum ramp rates are assigned in a top-down manner. Their total capacities as well as their dispatch are treated as optimization variables. Similar flexibility classes are also defined in Ref. [19], where a Fourier-like decomposition of the residual load is used to estimate flexibility requirements, but their model focuses on a optimal decommissioning of the currently installed capacities.

First discussions of the explicit impact of the dominant meteorological timescales on the required backup infrastructure of

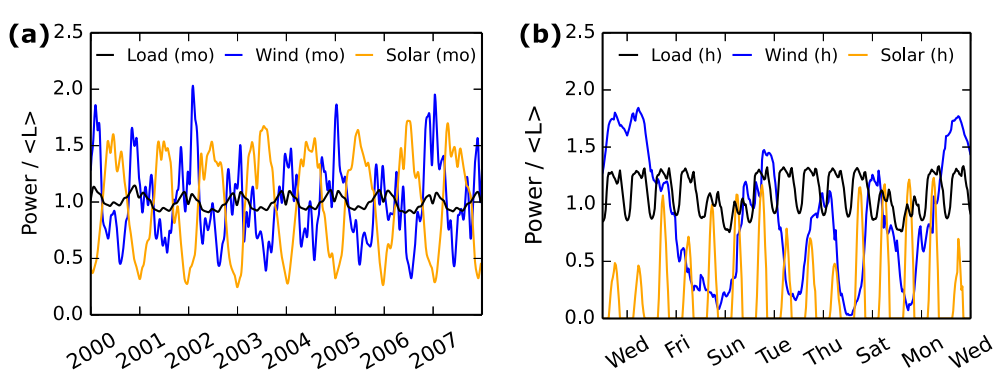

Fig. 1. Examples of time series of load and weather-based wind/solar generation in Germany based on data described by Heide et al. [1]. (a) All eight years of data, smoothed over one month to see long-term trends. (b) Hourly load and generation for two example weeks in October 2000. All time series have been normalized to an average load of one.

highly renewable large-scale electricity systems have recently been put forward. Heide et al. [1] discuss a seasonal optimal mix of wind and solar power, where the combined renewable power generation exactly follows the seasonal dependence of the load. They find that this greatly reduces the need for storage. In addition, Jensen and Greiner [20] show that the remaining required amount of storage is mainly determined by the fluctuations of the renewable power generation on the synoptic timescale. With the same modelling approach, Rodríguez et al. [21] and Becker et al. [22] estimate the transmission needs across a highly renewable European power system, highlighting the importance of large-scale transmission grid expansion. The balancing energy and power requirements have been addressed in [23,24]. However, all the balancing needs have been assumed to be only highly flexible. Different flexibility classes have not been discussed there, and will be the main focus of this study.

The model presented here uses the backup system as only source of flexibility. This simplified approach allows to assess the general trends of the flexibility requirements, and especially the optimal contribution of slowly flexible generators in the electricity sector if no other flexibility options are available. However, the model does not consider the impact of additional flexibility like storage and transmission to avoid the complex interplay between different flexibility options in more detailed models [17]. Nevertheless, it can be used to provide a basis for the quantification of the benefits of other options.

The paper is organized as follows: Section 2 describes the data base and the modelling approach. Further technical details of the model can be found in Appendix A. The main results are presented in Section 3, whereas model sensitivities to the physical parameters are shown in Section 4. The results as well as model assumptions and potential extensions are discussed in Section 5. Section 6 compares the decommissioning timescales of the optimized and installed slowly flexible capacities in Germany. Finally, Section 7 summarizes the conclusions and provides an outlook for further relevant research topics.

2. Methods

In this paper the power system model consists of variable renewable energy generation from wind and solar PV in combination with a dispatchable, conventional backup system that together balance the electricity consumption.

2.1. Data

The power generation data for wind and solar energy are based on historical weather data for 30 European countries covering the years 2000–2007 with time resolution of 1 h on a grid with a spatial resolution of about $50 \times 50\,\mathrm{km}^2$, as described in detail by Heide et al. [1]. There, the generation data were aggregated on country level, ignoring national transmission constraints. These authors also provided the corresponding national hourly energy consumption data as published by the transmission system operators [25]. Here, the time series for wind power generation $W(t)$, solar power generation $S(t)$, and consumption $L(t)$, are normalized to their mean $\langle W\rangle = \langle S\rangle = \langle L\rangle = 1$, where $\langle\cdot\rangle$ is the time average of a series.

Whenever the consumption is higher than the renewable generation, the remaining demand has to be covered by a backup system. This residual load $L_R(t)$ at each hour t is calculated as the positive part of the difference between consumption and renewable energy production:

$$L_R(t) = (L(t) - \gamma[\alpha W(t) + (1-\alpha)S(t)])_+ \tag{1}$$

where $\alpha \in [0,1]$ is the wind fraction in the relative share between wind and solar power generation, and γ is the VRES gross share, i.e. the average combined wind and solar power production in units of the mean load. For $\gamma = 1$, the average renewable generation equals the average consumption over the 8-year period. Here, $(X)_+ = \max(0, X)$ denotes the positive part of a quantity X. Similarly, $(X)_- = -\min(X, 0)$ is the negative part of X.

Throughout this paper, a fixed wind-solar ratio of $\alpha = 0.7$ is chosen for each country, which is a good approximation to the optimal mix that minimizes the average residual load [21].

2.2. Modelling dispatchables

The electricity system beyond load and VRES generation is modelled in a simplified fashion. It is assumed that VRES take precedence in covering the demand. Whenever VRES overproduction occurs, it is assumed to be curtailed. The residual load (cf. Eq. (1)) is covered by a dispatchable backup system in order to guarantee the security of supply. Storage is not included at this point. Working with country-aggregated time series, country-internal transmission bottlenecks are implicitly neglected. Only two limiting cases of power transmission are regarded: isolated countries, corresponding to zero cross-border transmission, or aggregated Europe, corresponding to unconstrained transmission. These cases provide bounds for a more detailed system with partly congested international transmission. The two reference cases here are Germany without international transmission and an aggregated Europe.

In order to study the flexibility requirements in more detail, the backup system is split into three flexibility classes, based on the timescales of the variations they cover. As seen in Fig. 1, the variations of load and renewable generation typically occur on the intra-day, synoptic, and seasonal timescales. The flexibility classes are therefore implemented into the model by splitting the dispatchable system into a daily, a synoptic, and a seasonal part. For each of these parts i, the maximum rate of change m_i of their power output B_i is limited. As the seasonally flexible part is the slowest and the daily flexible part the fastest, the three systems are also referred to as the fast, the medium, and the slow system. Furthermore, the power capacities of the three components are limited to K_i. Together, the dispatch of the three components is optimized in a way that minimizes excess and deficit of backup energy with small installed capacities and high utilization.

This is done by solving the optimization problem:

$$\min \Phi = \left[\underbrace{\sum_t \left(L_R(t) - \sum_i B_i(t)\right)^2}_{\text{match residual load closely}} + \underbrace{c\sum_i w_i K_i}_{\text{reduce power capacities}} + \underbrace{\frac{d}{T}\sum_{i,t} v_i B_i(t)}_{\text{increase utilization}}\right] \tag{2}$$

$$\text{subject to} \quad \left|\frac{\Delta B_i(t)}{\Delta t}\right| \leqslant m_i, \quad 0 \leqslant B_i(t) \leqslant K_i, \quad \text{with } i = \text{fast, medium, slow}; \quad t = 1, \ldots, T$$

where t runs over all $T = 70,128$ h of the 8 year time series. The parameters c, w_i in the second term are the relative weights of the capacities, with priority given to the less flexible classes. The latter is necessary to avoid the trivial optimum where only the most flexible system is used to perfectly match the demand. The last term determines the order in which the three systems are dispatched, via the weights d, v_i with which the usage of potential backup

energy production of class i is encouraged, leading to higher utilization of slower systems.

2.2.1. Parameter choices

2.2.1.1. Ramp rates. A lower bound on the ramp rates present in the current system can be inferred from the load data. The contribution of renewables in the years 2000–2007 was very low ($\gamma \approx 0$ [22]), and the conventional dispatchable power system thus covered the full load almost on its own. Therefore, the ramp rates m_i of the historic dispatch can be extracted from the load in the following way:

1. The maximum ramp rate m_{slow} of the slow system is set to the maximum slope of the load over the relevant timescale of one week. Before calculating the slopes, fluctuations on shorter timescales are suppressed by smoothing the load time series via convolution with a Gaussian kernel $\text{Ker}_\tau(t) = \sqrt{\pi/(2\tau^2)}\exp(-\pi^2 t^2/(2\tau^2))$ with a standard deviation of one week ($\tau = 168$ h), which replaces each load value by a weighted average of its neighbours. Therefore, $m_{\text{slow}} = \max\left(\left|\frac{\text{d}}{\text{d}t}(\text{Ker}_\tau * L)\right|\right)$, where L is the load time series, $f * g$ is the convolution of f and g, and $|\cdot|$ is the (element-wise) absolute function.
2. The maximum ramp rates m_{medium} of the weekly variations are then calculated in a similar way. To avoid contributions from variations on the longer timescales, the weekly smoothed load time series is subtracted from the load first, then only the remainder is convolved with a Gaussian of the width of one day ($\tau = 24$ h).
3. The fastest components are assumed to be flexible enough to follow the slope of the load at all times and therefore m_{fast} remains unconstrained.

The ramp rates are calculated from the load of each country separately, or in the aggregated case from the aggregated load over all countries. The m_i of the reference models are listed in Table 1. The given m_{medium} correspond to 54%/32%$\langle L\rangle$day^{-1} for Germany/aggregated Europe, and the m_{slow} to 42%/29%$\langle L\rangle$week^{-1}.

Even the least flexible power plants that are currently used for baseload production have technical constraints that allow them to change their power output, and even perform a cold start on relatively short timescales of less than 1–24 h. However, it is not economically and ecologically feasible to cycle typical baseload plants on a regular basis, as shown by Oates and Jaramillo [26] for a US case study and by Van den Bergh and Delarue [27] for a German market. It is therefore reasonable to limit their ramp rates as an effective means of including these economic and regulatory constraints.

2.2.1.2. Capacity weights. The only difference between the flexibility classes in the model is their maximum ramp rates. If the capacities were unconstrained, the fastest backup component could cover the load perfectly on its own without any need for the slower components. To avoid this trivial optimum, the capacity weights are set to $w_{\text{fast}} > w_{\text{medium}} > w_{\text{slow}}$. The weights w_i used in the reference model are listed in Table 1. The model is found to be relatively insensitive to the ratio of these parameters as will be discussed in Section 4.3.

Table 1
Parameters of the reference models Germany (DE) and aggregated Europe (Agg).

Class	$m_i[\%\langle L\rangle \text{h}^{-1}]$		w_i	v_i	c	d
	DE	Agg.				
Fast	Unlimited	Unlimited	1	1	40	0.1
Medium	2.26	1.34	0.5	0.5	40	0.1
Slow	0.25	0.17	0.25	0.25	40	0.1

2.2.1.3. Dispatch weights. In the reference scenario, the dispatch weights v_i are increased with the flexibility of the class as shown in Table 1, in order to increase the utilization of the slower systems, which generally require more full load hours to be economically feasible [26].

As a side effect, the degeneracy in the order of the dispatch at the hours when no component is needed to its full capacity is lifted by the weights v_i in the third term in Eq. (2). The first two terms in the optimization function determine the total hourly dispatch and the capacities of the three system types, but they do not provide a unique solution for the distribution of the dispatch of the three components. With the inclusion of the third term, the slower systems are preferred. Avoiding the degeneracy requires only a small weight for this term, and $d = 0.1$ was chosen as this was found in this study to best reproduce the typical dispatch characteristics of today's system.

2.2.1.4. Missing energy. The objective function Eq. (2) does not require a perfect match between demand and supply, but only aims at minimizing the uncovered load as well as excess production by the dispatchable systems. In practice this residual mismatch could be covered by a limited amount of load shedding and additional curtailment of renewable generation, respectively, or other means of load shifting, depending on the economics of the various measures. Allowing a small deficit in energy production removes the otherwise disproportionately large influence of a small amount of extreme load hours on the backup capacities. In the model, the total amount of energy E_{miss} that is not covered during the full range of the time series depends mostly on the capacity of the fastest backup component. The minimum amount of total covered energy was set to 99.97%, such that 20 average load hours (av.l.h.) are allowed to remain unserved over the course of the eight year time period. This can be done by setting the capacity weight $cw_{fast} = 40$, as discussed in the following. $E_{\text{miss}} = 20$ av.l.h. corresponds to full load coverage for about 99% of all hours at a renewable gross share of $\gamma = 30\%$. The number of uncovered hours as a function of γ is shown in Appendix A.1.

Numerically, it is observed that the amount of missing energy can be controlled by the weights cw_{fast} as:

$$E_{\text{miss}} = \sum_t \left(L_R(t) - \sum_i B_i(t)\right)_+ \approx \frac{cw_{fast}}{2} \tag{3}$$

where E_{miss} is measured in units of the mean hourly load $\langle L\rangle$. This can be understood by considering a variation of the optimization function with respect to the fast capacity K_{fast}. One can assume that in an uncovered hour all backup capacities are operated very close to full capacity, such that

$$\sum_t \left(L_R(t) - \sum_i B_i(t)\right)_+ \approx \sum_t \left(L_R(t) - \sum_i K_i\right)_+ \tag{4}$$

If the fast capacity is too small, a given E_{miss} can only be achieved by increasing slow or medium generation, which leads to considerable overproduction. Therefore, the optimization mainly seeks a trade-off between reducing the amount of uncovered energy and increasing the fast capacity. Denoting the optimization function by Φ and using the first part of (3), this trade-off can be approximated by

$$\begin{aligned}\frac{\delta\Phi}{\delta K_{fast}} &\approx \frac{\delta}{\delta K_{fast}}\left(\sum_t \left(L_R(t) - \sum_i K_i\right)_+^2 + c\sum_i w_i K_i\right) \\ &= -2E_{miss} + cw_{fast} \overset{!}{=} 0\end{aligned} \tag{5}$$

which yields the second part of (3).

In a similar way, the excess energy from the three flexible systems $E_{excess} = \sum_t (L_R(t) - \sum_i B_i(t))_-$ is determined by the slow capacity. The optimization in this case seeks to reduce the amount of excess energy by lowering the use of slow capacity. But less slow capacity also increases the amount of missing energy, since almost all of the capacity of the backup system is needed to cover the highest demands, as argued in the previous paragraph. The variation of Φ with respect to K_{slow} therefore influences both excess and missing energy, although in opposing manner, and in analogy to (5) can be well approximated by

$$\frac{\delta\Phi}{-\delta K_{slow}} \approx 2E_{miss} - 2E_{excess} - cw_{slow} \stackrel{!}{=} 0 \tag{6}$$

In combination with (3) this then yields

$$E_{\text{excess}} = \sum_t \left(L_R(t) - \sum_i B_i(t) \right)_- \approx \frac{cw_{fast}}{2} - \frac{cw_{slow}}{2} \tag{7}$$

which is also observed numerically as long as the weight d of the utilization term in Eq. (2) is as small as in the reference model. Since both E_{miss} and E_{excess} are only functions of the capacity weight parameters, they can be controlled independent of other model parameters like the maximum ramp rates or γ.

3. Results

3.1. Development of dispatchable capacities

The development of the optimal capacities of the modelled dispatchable backup systems for increasing gross shares γ of VRES is shown in Fig. 2 for Germany as an isolated country. The total required backup capacity $K_{\text{tot}} = \sum_i K_i$ (magenta line) does not decrease significantly from its initial value of $K_{\text{tot}} = 1.35$ in units of the mean load $\langle L \rangle$. It decreases only slightly to $K_{\text{tot}} = 1.16$ and 1.09 even for very high VRES gross shares $\gamma = 1$ and 2, respectively. At $\gamma = 0$, the dominant share of the backup capacity is contributed by the slowly flexible system (green line) with a capacity of $K_s = 0.88$. However, for larger γ K_s falls off significantly until it is below $K_s < 0.2$ for $\gamma > 0.5$. The capacity K_m of the medium flexible class (red line) starts for $\gamma = 0$ at $K_m = 0.2$, peaks to $K_m = 0.43$ at $\gamma = 0.35$, and drops below the initial value for $\gamma > 1$. The fast capacity (blue line) is almost constant at $K_f = 0.27$ for $\gamma < 0.2$, but then rapidly increases towards $K_f \approx 0.9$ for $\gamma > 1$.

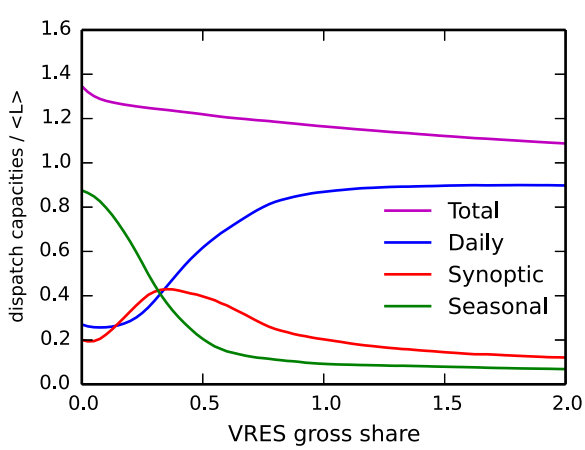

Fig. 2. Modelled optimal backup capacities in units of the mean load versus VRES gross share γ for Germany. The blue, red, and green lines correspond to the fast, medium, and slow flexibility classes, respectively. The sum of the three capacities is given by the magenta line. (For interpretation of the references to colour in this figure legend, the reader is referred to the web version of this article.)

These results can be intuitively understood with the help of the modelled dispatch of the three flexibility classes shown in Fig. 3 (a)–(c). All three panels show the same two week period as Fig. 1 (b), but at three different levels of VRES shares with $\gamma = 0, 0.5$, and 1, respectively.

For $\gamma = 0$ the VRES do not contribute and the backup system has to cover the full load. As the load varies only moderately around its mean in this case, the slowly flexible system is able to cover a large fraction of it, as indicated in Fig. 3(a). The remaining load especially during the weekends is small enough to be covered mostly by the medium system, while the fast system covers the fluctuations on shorter timescales. The slow and medium flexible systems are often used to their full capacities, especially during the winter months when the consumption is highest, in accordance with the optimization objective, as discussed in Section 3.3.

In the case of $\gamma = 0.5$, the situation changes significantly, as shown in Fig. 3(b). The high share of VRES leads to large fluctuations in the residual load. This includes hours with virtually unchanged maximum load that require the full backup capacity, but also hours with zero residual load when the VRES production is larger than the demand and has to be curtailed. Due to the large share of wind power in the mix of the renewables, these overproduction events typically happen on a synoptic timescale. The medium flexibility class is therefore well suited to follow these fluctuations, leading to the increase in K_m for relatively small $\gamma < 0.3$ shown in Fig. 2.

However, for larger shares of VRES additional overproduction events occur on even shorter timescales of hours to days, as indicated in Fig. 3(c). The medium system is then no longer flexible enough to follow most of these fast variations and its capacity decreases with γ as observed above. K_f is substantially increased as the fast system has to cover the large remaining variations.

The trends of the capacities at different γ described above agree qualitatively with the results reported by Tarroja et al. [7] for a case study of California's electricity system. These authors define comparable flexibility classes but use a purely statistical approach. They also find a sharp decrease of K_s from 13% to 50% renewable penetration, a slightly peaked K_{medium}, and an increase in K_s as function of γ. However, their model does not optimize capacities and results in a much smaller share of slow capacity in the initial system, compensated by a large share of fast capacity.

3.2. Aggregation benefits

In the previous section the case of an isolated German electricity system without transmission to other countries was discussed. Fig. 4 illustrates the benefits of unlimited transmission in an aggregated Europe, where excesses and residual loads are shared and exchanged. Here the total capacity decreases significantly with γ from 1.37 to 0.85 for $\gamma = 0$ to 1 and even further to 0.53 for a large over-installation of VRES with $\gamma = 2$. This is in contrast to the much slower decrease in the isolated case. Comparable benefits of large scale aggregation for the total required capacity and energy are also reported by e.g., [19].

In the aggregated case, K_s is higher by $\approx 0.1\langle L \rangle$ for $\gamma < 0.5$. This is due to the smoothing effect of spatial aggregation where opposing fluctuations in different regions cancel each other, leading to less extreme variations (see e.g., Ref. [8]). The smoother global residual load can therefore be better matched by the slow system. K_s approaches the small values observed for the isolated case for larger γ.

Since the slow system now covers more of the residual load, the capacities of the more flexible systems can be reduced. K_m is smaller by ≈0.1–0.15 in the aggregated case, relatively independent of γ. The maximum value is also decreased to 0.3 and shifted to a

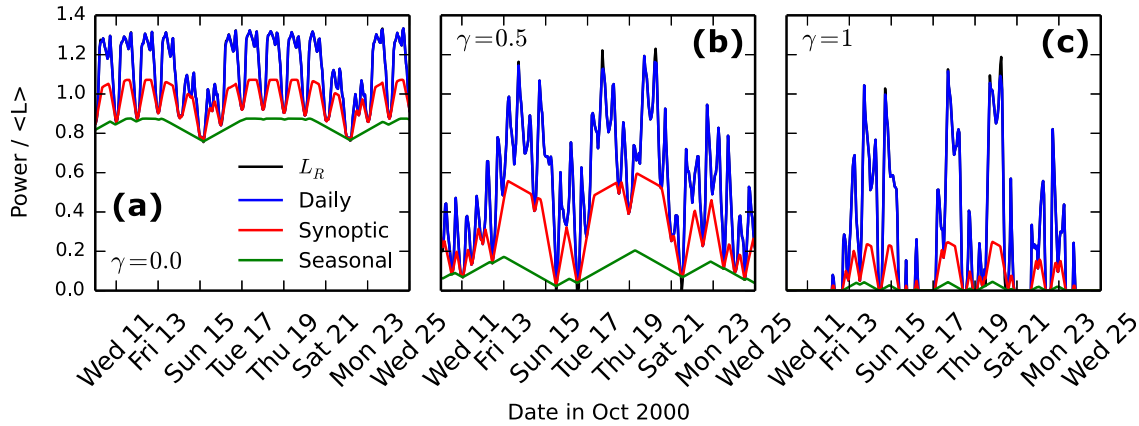

Fig. 3. A two-week period of the modelled dispatches for Germany for $\gamma = 0, 0.5, 1$ in panels (a,b,c), respectively. The dispatches of the slow, medium, and fast flexibility classes (green, red, blue lines) are plotted cumulatively, and together match the (residual) load (black lines, mostly overlapped by the blue lines) at almost all times. (For interpretation of the references to colour in this figure legend, the reader is referred to the web version of this article.)

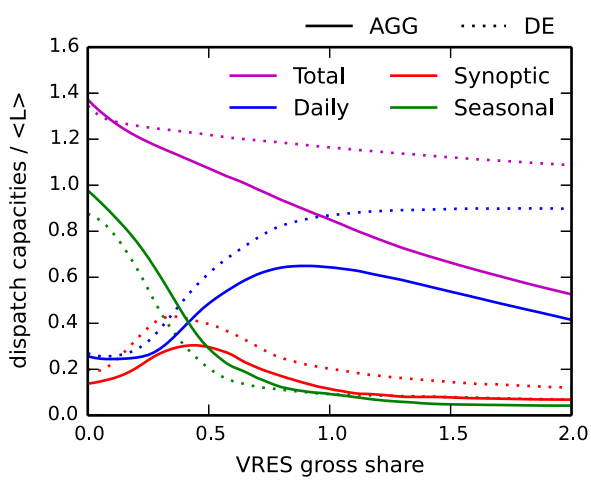

Fig. 4. Modelled capacities versus VRES gross share γ. Same as Fig. 2, but for aggregated Europe (solid) in addition to Germany (dotted).

slightly larger $\gamma = 0.45$, indicating that the spatially smoothed VRES generation allows a higher γ before significant fluctuations and curtailment events occur on the synoptic timescale.

For small γ the K_f in the aggregated system is similar to that of the isolated case, but it increases slower with γ and even reaches a maximum of $K_f = 0.65$ around $\gamma = 0.9$ after which it declines, following the decrease of the total required capacity.

The remaining part of this paper focuses on the case of an aggregated Europe because it allows the largest possible contributions from the slower system, and therefore allows to quantify an upper bound for their required capacities.

3.3. Slow capacities going out of use

The previous section quantified how fast the capacity of the slowly flexible class decreases with an increased share of VRES due to its limited ability to follow the volatile behaviour of the residual load. Since the model prefers the use of the slow system whenever possible, these capacities are an upper bound. However, Fig. 3 indicated that for VRES gross shares larger than about $\gamma > 50\%$ these capacities cannot often be used to their full extent. This is quantified by the utilization fraction f_i defined as the ratio

$$f_i = \frac{\langle B_i \rangle}{K_i} \tag{8}$$

between the mean hourly dispatch $\langle B_i \rangle$ and capacity K_i. Fig. 5(a) shows f_i as a function of γ. As is typical for baseload systems, the slow system is highly utilized with $f_i \approx 80\%$ for small γ. However, with increased γ its average usage rapidly falls off due to more frequent and longer ramping. Only 50% of its capacity is used on average at $\gamma = 0.5$, and less than 10% as soon as $\gamma = 1$.

In combination with the decrease of its capacity K_f shown in Fig. 4, this results in a substantial reduction in the amount of average dispatch $\langle B_s \rangle$ generated per hour by the slow system. Initially, the contribution of the slow system is large with $\langle B_s \rangle = 80\%$ of the mean load $\langle L \rangle$, as shown in Fig. 5(b). But already at $\gamma = 50\%$ the slow system has a lower average dispatch than the other two systems. Here $\langle B_s \rangle = 15\%$ which corresponds to just 30% of the total average dispatch. At $\gamma = 100\%$, $\langle B_s \rangle$ is negligible in absolute as well as in relative terms.

Even though the use of the slow system falls off quickly with the share of renewable generation, the medium flexible system is able to compensate for some of the emerging fluctuations in the residual load at intermediate shares of VRES around $\gamma = 50\%$. Together with the increase in medium capacity, its utilization fraction increases slightly in these scenarios. This leads to a peak in the mean dispatch around $\gamma = 50\%$ where the medium system also contributes roughly one third of the dispatch. For larger γ its utilization fraction remains highest and is still $f_m = 25\%$ at $\gamma = 100\%$, resulting in a mean dispatch of 20% for the total system.

The fast flexibility class is designed to quickly react to the strongest demand fluctuations that cannot be covered by the slower systems. The utilization fraction of the fast system is therefore not expected to be very large. Indeed, the utilization f_f stays below 40% and declines even further for large γ even though it produces the largest share of backup energy for $\gamma > 0.5$, see Fig. 5(b).

The mean dispatch of the total system decreases from 100% proportional to the increasing gross share of the VRES until $\gamma \approx 0.6$, indicating that most of the VRES generation is used. For larger γ curtailment begins to play a significant role, such that more installation of VRES leads to less than an equivalent reduction in required backup energy. Most of the power at large $\gamma > 1$ therefore has to be covered by the fast system.

These results are also reflected in the dispatch duration curves of the backup systems for the three cases of $\gamma = 0, 0.5, 1$ shown in Fig. 6. A dispatch duration curve shows the fraction of time the dispatch of a given class equals or exceeds a certain value, or

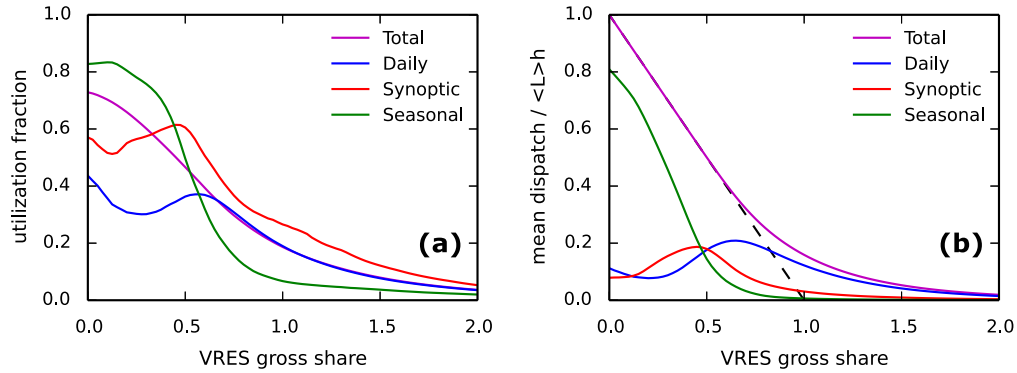

Fig. 5. (a) Utilization fractions f_i of the total, fast, medium, and slow systems (magenta, blue, red, green lines), respectively, as a function of the VRES gross share γ for aggregated Europe. (b) Mean hourly dispatch $\langle B_i \rangle_t = K_i f_i$ in units of the mean load $\langle L \rangle$ as a function of γ (same colour code as in (a)). The dashed black line marks the 1:1 correlation between the increase of contributions from the VRES and the corresponding decrease of the total residual demand. (For interpretation of the references to colour in this figure legend, the reader is referred to the web version of this article.)

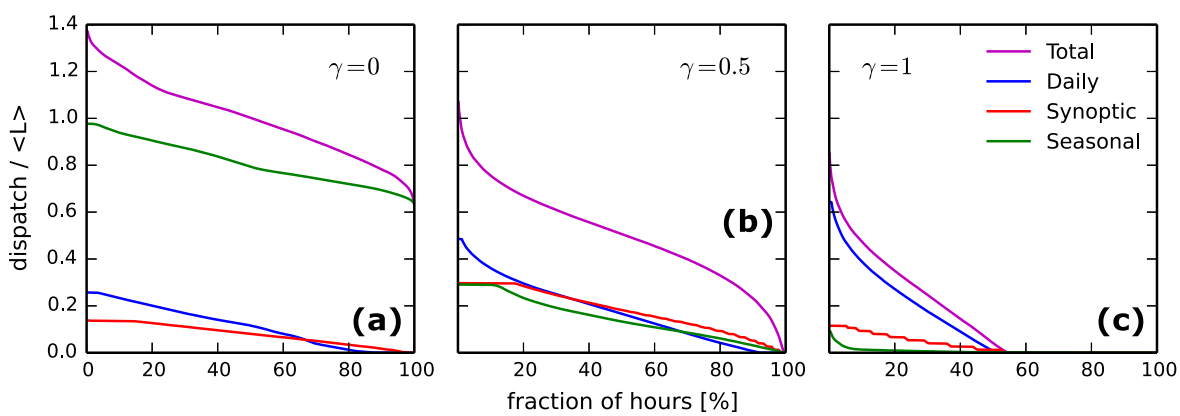

Fig. 6. Dispatch duration curves for the three flexibility classes and their sum at $\gamma = 0, 0.5, 1.0$ (a,b,c), which show the hourly dispatch not in chronological, but in decreasing order against quantiles of hours. Here 100% of the hours correspond to the 8 years of data.

equivalently, the hourly dispatch in decreasing order instead of in chronological order.

Fig. 6(a) shows the baseload properties of the slow system at $\gamma = 0$, as its dispatch never drops below 62%$\langle L \rangle$ and is able to follow the dominant slow seasonal variations. The total dispatch is equivalent to the demand over the time range. The total dispatch duration curve is much less peaked initially than in scenarios with higher VRES shares. At $\gamma = 0.5$ only a small fraction of hours is responsible for the highest need for backup generation, and therefore for the total capacity.

Fig. 6(b) also shows the onset of events with very low or zero residual load, i.e. the occurrence of a few hours when no dispatchable generation is needed. As indicated before, this is related to the increase of fluctuations of the residual load and can be associated with the significant decrease in capacity and utilization of the slow system. The modelling choice to prefer slow dispatch whenever possible leads to different shapes of the dispatch duration curves for the three classes. The slow and medium systems are run at full capacity for 10% and 20% of the time, respectively, as indicated by the horizontal parts of the lines in Fig. 6(b). However, the full capacity of the fast system is required only for a few extreme events. For about 10% of the time the fast system is not needed even though the total demand is almost never zero. This is mostly due to periods with little residual load when the medium system can cover the remaining fluctuations.

For $\gamma = 1$, the VRES generation satisfies the demand for about 45% of the time, as shown in Fig. 6(c). The residual load is also so volatile that it has to be covered almost entirely by the fast system, with some support from the medium class. The steps in the dispatch duration of the medium system are due to repeated up and down ramping from zero with the maximum rate while trying to cover short but relatively large peaks in the residual load that only last a few hours. The height of the steps is therefore a multiple of the ramp rate $m_m \times 1$ h. The slow class is used for only a small fraction of hours in this case even though the capacity is already strongly reduced.

4. Model sensitivities

4.1. Power capacities

The relatively low utilization fractions especially for larger shares of renewables discussed in the previous Section 3.3 suggest that it might be possible to reduce the optimal capacities slightly without increasing the amount of the missing energy E_{miss} dramatically. This was tested by fixing the capacities K_i of two flexibility classes to their optimal values for a given γ while reducing the capacity of the third class in small steps of $0.025\langle L \rangle$. After optimizing the dispatch of the three systems according to the objective function (2) again, but with these fixed K_i, the resulting $E_{\text{miss}} = \sum_t (L_R - \sum_i B_i)_+$ can be calculated.

The results are shown in Fig. 7(a) for capacities that result in $E_{\text{miss}} = 20$–70 av.l.h. in eight years, i.e. starting from the initial 99.97% covered energy and decreasing one capacity only until 99.9% of the energy is covered. The latter corresponds to full cover-

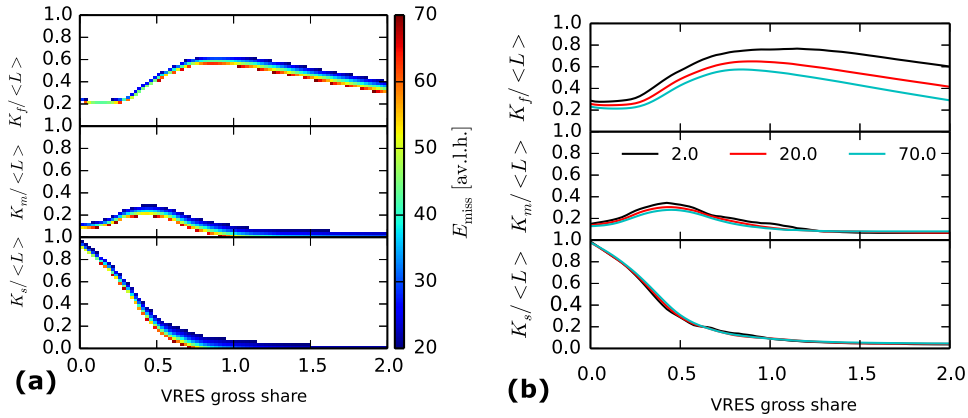

Fig. 7. (a) Sensitivity of missing energy E_{miss} to the reduction of one of the fast, medium, slow (top to bottom) capacities while the other two are fixed at their optimum value, as a function of γ for aggregated Europe. Colour-coded is E_{miss} in units of av.l.h. in eight years. In the white areas above/below, E_{miss} is lower/higher than the colour range. (b) Sensitivity of the capacities of the fast, medium, slow systems (top to bottom) on the allowed missing energy for $E_{miss} = 2, 20, 70$ av.l.h. over eight years (black, red, cyan lines) as function of γ for aggregated Europe. (For interpretation of the references to colour in this figure legend, the reader is referred to the web version of this article.)

age of the demand for roughly 97% of all hours at $\gamma = 0.3$. In the top panel, only the capacity K_f of the fast component gets reduced, but this quickly results in a total $E_{miss} > 70$ av.l.h., especially at small γ. Since the fast systems are dispatched last and their capacity largely determines the amount of E_{miss}, this shows that the optimized solution is robust, because small deviations from the optimum K_f lead to a large change in E_{miss} and in the objective function.

The capacity of the medium system (middle panel) can be lowered slightly more, from $K_m = 0.275\langle L\rangle$ to $0.175\langle L\rangle$ at $\gamma = 0.5$, without increasing E_{miss} above 70 av.l.h. because the fast systems can compensate occasionally by increasing their utilization fraction. This also shows that the capacities for the slower flexible systems is an upper bound, and the third term in the optimization function is important to control the dispatch order. If varying the slow capacity (bottom panel), $E_{miss} > 70$ av.l.h. is only reached once K_s is smaller than its optimum value by up to $0.2\langle L\rangle$ at $\gamma \approx 0.5$–0.7, e.g., by decreasing K_s from $0.2\langle L\rangle$ to $0.05\langle L\rangle$ at $\gamma = 0.6$. This also means that K_s can be set to zero for $\gamma > 0.7$, i.e. decommissioning of all slow capacities, without reducing the total amount of covered energy below 99.9%, if the other two systems are at their optimum capacities. The medium capacity (middle panel) can only be reduced to zero in this way while $E_{miss} < 70$ av.l.h. for large $\gamma > 0.9$.

4.2. Missing energy

In Fig. 7(b) the previous analysis is reversed: E_{miss} is fixed via Eq. (3) and the mix of backup capacities is optimized for different γ. Mainly the capacity of the fast system shown in the top panel reacts to an increased tolerance for E_{miss}. K_f decreases from 80% to $50\%\langle L\rangle$ at $\gamma = 1$ between $E_{miss} = 2$ and 70 av.l.h. in eight years. The capacities of the less flexible systems change much less, only K_m decreases slightly by less than $0.07\langle L\rangle$ for $\gamma < 1$. This supports the previous finding that the largest capacities are mostly required to cover a few events on a short timescale.

4.3. Ramp rates

Another important aspect of the model are the ramp rates that were chosen to match the typical timescales of variations in the renewable generation and consumption, see Section 2. In order to assess the sensitivity of the results to these parameters, Fig. 8 compares the modelled capacities assuming half and twice the ramp rates, respectively. Only the flexibilities of the medium and slow systems were changed, and the fast system is still assumed to be unconstrained.

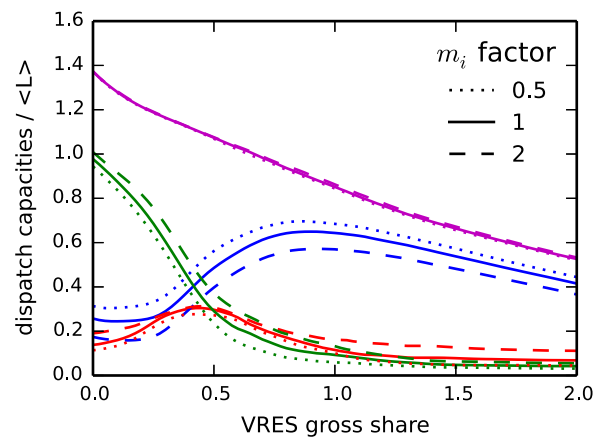

Fig. 8. Modelled capacities assuming half (dotted) and twice (dashed) the reference (solid) ramp rates (m_f remain unconstrained), respectively, versus γ for aggregated Europe. Total, fast, medium, slow capacities are shown as magenta, blue, red, green lines. Solid lines are the same as in Fig. 4. (For interpretation of the references to colour in this figure legend, the reader is referred to the web version of this article.)

The total capacities are virtually unchanged in all cases as only the relative mix between the capacities changes. If larger ramp rates are assumed, the slow system can contribute more and K_s increases by 0.04–$0.06\langle L\rangle$ for $\gamma < 1$. The largest differences are around $\gamma = 0.5$–0.7 where the benefits are greatest for a more flexible slow system that is able to ramp up and down between the increasing number of events with zero residual load. The reversed argument holds for the case with only half the reference ramp rates, leading to slightly decreased K_s for all γ. The differences in K_m are very small, especially around its peak at $\gamma = 0.5$. This suggests that most of the benefits of increased ramp rates can be used by the slow class, except at very small and large γ. As the capacity of the fast class is mostly influenced by the need to reduce missing energy, K_f adapts to the changes of the other capacities accordingly, and is higher and lower relatively independent of γ if the other systems are less and more flexible, respectively. Overall, the capacities are relatively insensitive to the choice of the ramp rates as higher flexibilities lead to a slight shift from fast to slow capacities, but the qualitative results remain unchanged.

Missing and excess energy of the optimized system are not influenced by variations of the maximum ramp rate, as they only depend on the capacity weights in accordance with Eqs. (3) and (7) in Section 2.2.1.

5. Discussion

Some aspects of the simplified model deserve some attention. First, there is the issue of the missing energy that is allowed for. The current electricity supply is designed for much higher security of supply than assumed in this paper. However, the treatment here can be justified by considering a backup system as only one part of an electricity supply complementing VRES. It is likely that future energy systems become more flexible, including new mechanisms like storage and demand-side management, simply because it is more economical to use these other options than to cover each and every demand as if it were a static boundary condition [28]. In such an environment, it is likely that there will be means to control those extreme hours not yet covered by the dispatchable backup system.

Furthermore, the ramp rates in this study are well below the technical limits of typical power plants [26]. They are chosen to effectively model the whole inertia in plant dispatch, which is not only due to technical constraints, but also to regulatory and economic conditions. Therefore, a slow capacity of zero does not necessarily mean that all slowly flexible power plants have to be shut down. Rather, these plants can still operate, but with shorter notification times, more cycling, and fewer full load hours, such that they would fall into the medium flexibility class in the terminology of this paper. This upgrade of already existing slow plants could also be an economically viable way to at least partly cover the $\gamma \approx 0.3$–0.5 peak of medium flexible capacity. Detailed economic feasibility studies of flexibility upgrades e.g., via enabling fuel switching in power plants support this assumption [29]. However, a clear trend towards more flexible power plants remains.

Sub-hourly fluctuations in consumption and VRES generation are not covered in the model. However, the wind generation power spectrum suggests that hourly/multi-hour fluctuations are dominant (i.e. stronger than sub-hour) [30] and therefore additional capacity needs to cover high-frequency fluctuations can be expected to be small, especially if aggregation benefits at least at a regional level can be assumed [31].

6. Comparison to the current German system

The optimal slowly flexible capacity decreases strongly from the dominant system component to almost zero contribution with increasing share of renewable generation. This suggests a large shift of the current power plant portfolio away from slow flexibility. A timescale for this modelled shift can be approximated by mapping values of the renewable gross share γ to years in the future, even though the model was not designed to optimize a pathway solution. This mapping is based on a logistic fit to historic and targeted wind and solar PV penetrations in Germany for the years 1990–2050, as described by Becker et al. [22]. These authors use the 2020 targets defined in Germany's National Renewable Energy Action Plan [2], and assume $\gamma = 100\%$ for 2050. The optimized capacities as a function of time are shown in Fig. 9.

In order to assess the impact of this shift in the currently installed generator fleet, the expected remaining lifetime of the slowly flexible capacity in Germany is estimated as described in the following. From the complete list of German power plants provided by Bundesnetzagentur [32], all nuclear, lignite and coal power plants that are older than 10 years, i.e. built before 2004, are included. More recently installed or renovated plants are assumed to be already capable of a more flexible efficient operation. If these slowly flexible power plants would be decommissioned after a fixed economic lifetime of $n = 30$, 35, or 40 years, the remaining installed capacity as function of time is also shown in Fig. 9. Some of the generators already operate longer than 40 years without major renovation and would be decommissioned immediately in this scenario.

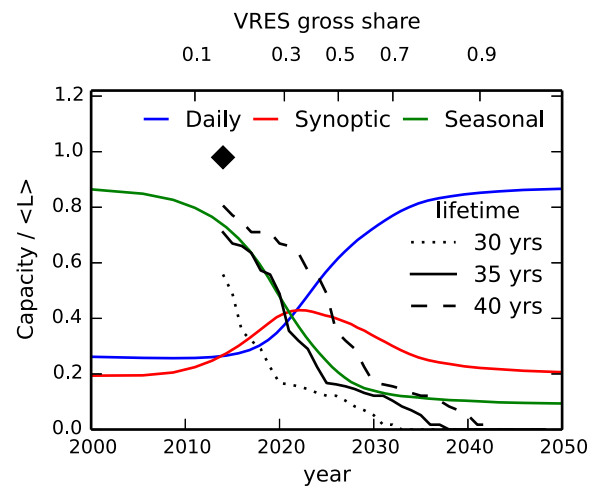

Fig. 9. Comparison between the modelled and estimated remaining slowly flexible capacities in isolated Germany as function of time. The modelled slow, medium, and fast (green, red, blue lines) capacities are the same as in Fig. 2 but with the VRES gross share transformed to years as described in the text. The black lines show the expected decommissioning of currently installed slowly flexible nuclear, lignite, and coal power plants in Germany if lifetimes of either 30, 35, or 40 years (dotted, solid, dashed lines) are assumed. Their current (2014) capacity without decommissioning is marked by the black diamond. (For interpretation of the references to colour in this figure legend, the reader is referred to the web version of this article.)

Under these assumptions, the decrease of the optimized slow capacity in Germany happens on a similar timescale as the end of economic lifetime decommissioning of installed capacity, especially for an assumed lifetime of 35 years. This implies that in this scenario where electricity production is the only source of flexibility, no additional slowly flexible generators should be built. It also suggests that most of these generators can be utilized until the end of their economic lifetime, if favourable conditions are assumed, and do not have to be decommissioned ahead of time.

7. Conclusions and outlook

A simplified capacity and dispatch optimization model of the European power system was used to determine the amount of VRES gross share γ above which power plants can no longer be run in baseload mode. An important contrast to bottom-up models with individual plants is that this model is independent of the details of the dispatchable power plant fleet, such as the plant number–size distribution or the detailed ramp potentials of individual power plants in different states. As seen in Section 4 and Appendix A, the results are stable under changes in the physico-technical assumptions as well as the weight parameters of the model.

For isolated countries, the phase-out of slowly flexible capacities comes at about $\gamma \approx 50\%$, for aggregated Europe, at about $\gamma = 50$–70%. From then on, power plants that today are used for baseload requirements will have to be run in a higher flexibility class – or be decommissioned if this is not economically and/or ecologically feasible. This increases the demand for plants that are more efficient and more economical when cycled regularly.

The need for medium flexible plants first rises in parallel with the decrease in need for baseload plants, until it peaks at $\gamma = 35\%$ and $\gamma = 45\%$ for isolated countries and aggregated Europe, respectively. This is due to the growing fluctuations in the residual load on the synoptic timescale that can be followed by the medium flexible class. For higher γ, the typical fluctuation timescales

become too short for the medium system, so that it can support the fast system decreasingly well until it contributes only 20% of the energy at $\gamma = 100\%$.

In contrast, the highly flexible capacity is seen to rise sharply, once the fluctuations of the residual load become too large for the slower systems. The capacity goes up from 30% of the average load to 50% and 60% at $\gamma = 50\%$ and further up to 65% and 85% at large $\gamma = 100\%$, for the aggregated and isolated cases, respectively. At that point it is used to cover almost the entire residual load in both cases.

If countries are regarded as isolated entities, the total power capacity of the dispatchable system is seen to decrease by only 19%, even at an extreme VRES gross share of $\gamma = 200\%$. Here, Europe-wide sharing of dispatchable resources could significantly reduce the requirements by about 60% at $\gamma = 200\%$.

Nonetheless, the large and rarely needed capacities still pose severe problems. In order to reduce these capacities further, a future energy system should be considered that includes storage and demand-side-management within the electricity sector, as well as couplings to other energy sectors, similar to those proposed in e.g., Ref. [14], where the electricity sector is coupled to heating/-cooling via heat pumps and power-to-gas, and to the transport sector by electric vehicles and electrically generated synfuels (see also [15]). This is also expected to increase the relative share of slowly flexible systems due to considerably reduced fluctuations in the residual load. These couplings will be investigated in a future extension of the model. Beyond that, limited transmission will be included to interpolate between the two extreme cases of isolated countries and an aggregated continent. Furthermore, the uncertainties associated with limited prediction horizons and forecast errors will also be included. All of these considerations will help to develop a new and efficient planning tool for emerging large-scale renewable electricity systems.

Acknowledgements

The authors thank Mirko Schäfer, Tom Brown, and Jonas Hörsch for helpful discussions, and the anonymous reviewers for their helpful suggestions and comments that improved this work. The project underlying this report was supported by the German Federal Ministry of Education and Research under Grant No. 03SF0472C. The responsibility for the contents lies with the authors.

Appendix A. Modelling details

A.1. Unserved hours

One important aspect of the modelling approach is to allow for a small amount of mismatch between residual load and the backup dispatch. The relation $E_{\text{miss}} = \frac{cw_{fast}}{2}$ in Eq. (3) gives a good handle for the control of the unserved energy. The reference value of E_{miss} was chosen to guarantee security of supply, i.e. exact residual load matching, for approximately 99% of all hours. For that, an hour is defined to be unserved if the total dispatch is smaller than the demand by $L_R(t) - \sum_i B_i \leqslant 10^{-4}\langle L\rangle$ in order to avoid numerical artefacts. The quantile $q = 1 - \frac{N_{miss}}{T}$ of fully covered hours is then calculated from the number of partially unserved hours N_{miss} over the full time range T of the data.

Fig. A.10 shows q as a function of γ for given E_{miss}. It indicates that for small shares of renewables there are few extreme outliers in the demand and the allowed amount of mismatch can be distributed over many hours. However, with increasing γ there is a concentration of the missing energy to fewer, more extreme hours. For higher E_{miss} the number of unserved hours also increases. At the reference value $E_{\text{miss}} = 20$ av.l.h. security of supply is given for at least a quantile of $q > 99\%$ for all $\gamma > 30\%$.

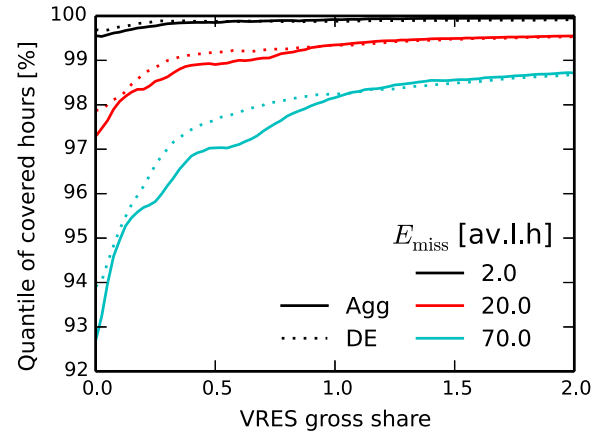

Fig. A.10. Quantiles of the number of covered hours at $E_{\text{miss}} = 2, 20, 70$ av.l.h. in eight years (black, red, cyan) as a function of VRES gross share γ for aggregated Europe (solid) and isolated Germany (dotted). (For interpretation of the references to colour in this figure legend, the reader is referred to the web version of this article.)

The effect of aggregation is not very large in this case. The allowed E_{miss} is distributed over slightly more hours around $\gamma = 0.5$ in the aggregated case, indicating a smoother residual load. But at larger γ the most extreme events occur also on a large spatial scale and are not easily mitigated just by transmission.

A.2. Sensitivity to capacity weights

The relative weights w_i of the capacities K_i where chosen such that the fast class has the largest weight, i.e. K_f is as small as possible. If the ratio between the w_i is not set to $w_f : w_m : w_s = 4 : 2 : 1$ as in the reference model, but to $100 : 10 : 1$, i.e. the weight of the fast class is even more dominant, the quantitative results change slightly, but the qualitative behaviour is the same, as shown in Fig. A.11. The major difference is that the fast capacity is decreased only slightly by less than $0.03\langle L\rangle$. But since the amount of allowed uncovered energy E_{miss} is still the same, the medium and slow capacities have to be increased over-proportionally by up to

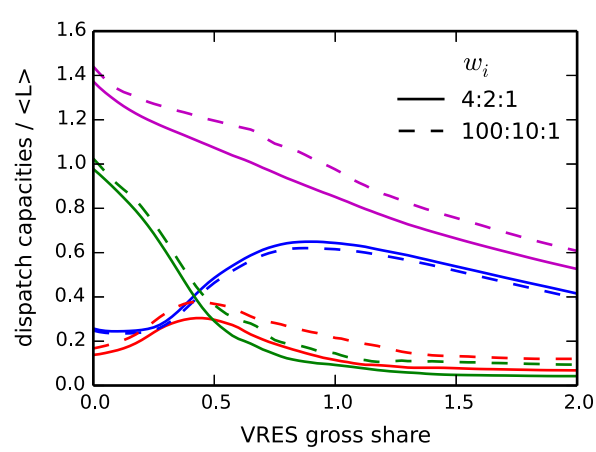

Fig. A.11. Modelled capacities assuming relative ratios of the capacity weights $w_f : w_m : w_s = 4 : 2 : 1$ (solid, reference model) and $100 : 10 : 1$ (dashed) versus γ for aggregated Europe. Total, fast, medium, slow capacities are shown as magenta, blue, red, green lines. Solid lines are the same as in Fig. 4. (For interpretation of the references to colour in this figure legend, the reader is referred to the web version of this article.)

$0.1\langle L\rangle$ and $0.09\langle L\rangle$, respectively, to provide the same security of supply for a few more extreme hours. The total capacity therefore is also larger by up to $0.15\langle L\rangle$. Not shown, the amount of overproduced energy increases and the utilization fraction decreases as the less flexible systems are less efficient in reaching the peaks of the residual load that were covered before by the additional capacity of the very flexible fast system.

A.3. Sensitivity to dispatch weights

The model optimization shows that the relative weights v_i in the utilization term in the objective function (2) do not influence the quantitative results, as the differences between the reference ratios $v_f : v_m : v_s = 4 : 2 : 1$, and $100 : 10 : 1$ are negligible. This is expected because this term was mainly intended to lift the degeneracy in the dispatch order for a given capacity mix, and therefore has a small weight d. In this case a reversed order of the weights would not change the optimal capacities, but dramatically reduce the utilization fraction of the medium and slow components in favour of the fast system.

References

[1] Heide D, von Bremen L, Greiner M, Hoffmann C, Speckmann M, Bofinger S. Seasonal optimal mix of wind and solar power in a future, highly renewable Europe. Renew Energy 2010;35:2483–9. http://dx.doi.org/10.1016/j.renene.2010.03.012.

[2] EU member countries. National renewable energy action plans; 2010. <http://ec.europa.eu/energy/renewables/action_plan_en.htm> [accessed Feb 2016].

[3] Holttinen H. Hourly wind power variations in the nordic countries. Wind Energy 2005;8(2):173–95. http://dx.doi.org/10.1002/we.144.

[4] IEA. Harnessing variable renewables – a guide to the balancing challenge. Tech. Rep. Paris: International Energy Agency; 2011.

[5] Ma J, Silva V, Belhomme R, Kirschen DS, Ochoa LF. Evaluating and planning flexibility in sustainable power systems. In: IEEE power and energy society general meeting (PES), 2013 IEEE. IEEE; 2013. p. 1–11. http://dx.doi.org/10.1109/PESMG.2013.6672221.

[6] Jones LE, editor. Renewable energy integration – practical management of variability, uncertainty, and flexibility in power grids. London Waltham San Diego: Academic Press; 2014.

[7] Tarroja B, Mueller F, Eichman JD, Samuelsen S. Metrics for evaluating the impacts of intermittent renewable generation on utility load-balancing. Energy 2012;42(1):546–62. http://dx.doi.org/10.1016/j.energy.2012.02.040. 8th world energy system conference, {WESC} 2010.

[8] Huber M, Dimkova D, Hamacher T. Integration of wind and solar power in Europe: assessment of flexibility requirements. Energy 2014;69:236–46. http://dx.doi.org/10.1016/j.energy.2014.02.109.

[9] Lannoye E, Flynn D, O'Malley M. Evaluation of power system flexibility. IEEE Trans Power Syst 2012;27(2):922–31. http://dx.doi.org/10.1109/PESGM.2012.6345375.

[10] Ulbig A, Andersson G. On operational flexibility in power systems. In: IEEE power and energy society general meeting, 2012 IEEE. IEEE; 2012. p. 1–8. http://dx.doi.org/10.1109/PESGM.2012.6344676.

[11] Ulbig A, Andersson G. Analyzing operational flexibility of electric power systems. Int J Electr Pow Energy Syst 2015;72:155–64. http://dx.doi.org/10.1016/j.ijepes.2015.02.028. the special issue for 18th power systems computation conference.

[12] Weitemeyer S, Kleinhans D, Vogt T, Agert C. Integration of renewable energy sources in future power systems: the role of storage. Renew Energy 2015;75:14–20. http://dx.doi.org/10.1016/j.renene.2014.09.028.

[13] Steinke F, Wolfrum P, Hoffmann C. Grid vs. storage in a 100% renewable Europe. Renew Energy 2013;50:826–32. http://dx.doi.org/10.1016/j.renene.2012.07.044.

[14] Mathiesen BV, Lund H, Conolly D, Wenzel H, Østergaard P, Möller B, et al. Smart energy systems for coherent 100% renewable energy and transport solutions. Appl Energy 2015;145:139–54. http://dx.doi.org/10.1016/j.apenergy.2015.01.075.

[15] Schiebahn S, Grube T, Robinius M, Tietze V, Kumar B, Stolten D. Power to gas: technological overview, systems analysis and economic assessment for a case study in Germany. Int J Hydrogen Energy 2015;40(12):4285–94. http://dx.doi.org/10.1016/j.ijhydene.2015.01.123.

[16] Schaber K, Steinke F, Hamacher T. Transmission grid extensions for the integration of variable renewable energies in Europe: who benefits where? Energy Policy 2012;43:123–35. http://dx.doi.org/10.1016/j.enpol.2011.12.040.

[17] Kondziella H, Bruckner T. Flexibility requirements of renewable energy based electricity systems – a review of research results and methodologies. Renew Sustain Energy Rev 2016;53:10–22. http://dx.doi.org/10.1016/j.rser.2015.07.199.

[18] Østergaard PA. Reviewing energyplan simulations and performance indicator applications in energyplan simulations. Appl Energy 2015;154:921–33. http://dx.doi.org/10.1016/j.apenergy.2015.05.086.

[19] Andresen GB, Rasmussen MG, Rodríguez RA, Becker S, Greiner M. Fundamental properties of and transition to a fully renewable pan-European power system. 2nd european energy conference, vol. 33. p. 04001. http://dx.doi.org/10.1051/epjconf/20123304001.

[20] Jensen TV, Greiner M. Emergence of a phase transition for the required amount of storage in highly renewable electricity systems. Eur Phys J Spec Top 2014;223(12):2475–81. http://dx.doi.org/10.1140/epjst/e2014-02216-9.

[21] Rodríguez RA, Becker S, Andresen GB, Heide D, Greiner M. Transmission needs across a fully renewable European power system. Renew Energy 2014;63:467–76. http://dx.doi.org/10.1016/j.renene.2013.10.005. preprint available at:Available from: <http://arxiv.org/abs/1306.1079>.

[22] Becker S, Rodríguez RA, Andresen GB, Schramm S, Greiner M. Transmission grid extensions during the build-up of a fully renewable pan-European electricity supply. Energy 2014;64:404–18. http://dx.doi.org/10.1016/j.energy.2013.10.010. preprint available at:Available from: <http://arxiv.org/abs/1307.1723>.

[23] Heide D, Greiner M, von Bremen L, Hoffmann C. Reduced storage and balancing needs in a fully renewable European power system with excess wind and solar power generation. Renew Energy 2011;36:2515–23. http://dx.doi.org/10.1016/j.renene.2011.02.009.

[24] Rasmussen MG, Andresen GB, Greiner M. Storage and balancing synergies in a fully or highly renewable pan-European power system. Energy Policy 2012;51:642–51. http://dx.doi.org/10.1016/j.enpol.2012.09.009.

[25] ENTSO-E. Country-specific hourly load data; 2011. <https://www.entsoe.eu/data/data-portal/consumption/>.

[26] Oates DL, Jaramillo P. Production cost and air emissions impacts of coal cycling in power systems with large-scale wind penetration. Environ Res Lett 2013;8(2):024022. http://dx.doi.org/10.1088/1748-9326/8/2/024022.

[27] Van den Bergh K, Delarue E. Cycling of conventional power plants: technical limits and actual costs. Energy Convers Manage 2015;97:70–7. http://dx.doi.org/10.1016/j.enconman.2015.03.026.

[28] Jansen M, Richts C, Gerhardt N, Lenk T, Heddrich M-L. Strommarkt-Flexibilisierung: Hemmnisse und Lösungskonzepte. Tech. Rep., Fraunhofer-Institut für Windenergie und Energiesystemtechnik (IWES), Energy Brainpool GmbH & Co. KG; 2015. Available at: <http://www.energybrainpool.com/services/studienverzeichnis.html> [accessed Mar 2015].

[29] Varympopiotis G, Tolis A, Rentizelas A. Fuel switching in power-plants: modelling and impact on the analysis of energy projects. Energy Convers Manage 2014;77:650–67. http://dx.doi.org/10.1016/j.enconman.2013.10.032.

[30] Apt J. The spectrum of power from wind turbines. J Pow Sources 2007;169(2):369–74. http://dx.doi.org/10.1016/j.jpowsour.2007.02.077.

[31] Fertig E, Apt J, Jaramillo P, Katzenstein W. The effect of long-distance interconnection on wind power variability. Environ Res Lett 2012;7:034017. http://dx.doi.org/10.1088/1748-9326/7/3/034017.

[32] Bundesnetzagentur. Kraftwerksliste; 2014. <http://www.bundesnetzagentur.de/cln_1432/DE/Sachgebiete/ElektrizitaetundGas/Unternehmen_Institutionen/Versorgungssicherheit/Erzeugungskapazitaeten/Kraftwerksliste/kraftwerksliste-node.html> [accessed Oct 2014].